Supporting information for:

Selection of Adlayer Patterns of 1,3-Dithia Derivatives of Ferrocene by the Nature of Solvent

Prithwidip Saha,[†] Vinithra Gurunarayanan,[†] Vladimir V. Korolkov,[‡] Prema G. Vasudev,[¶] Ramesh Ramapanicker,[†] Peter H. Beton,[‡] and Thiruvancheril G. Gopakumar[*,†]

[†]*Department of Chemistry, Indian Institute of Technology Kanpur, Kanpur, UP–208016, India*

[‡]*School of Physics and Astronomy, The University of Nottingham, Nottingham– NG7 2RD, UK*

[¶]*Molecular and Structural Biology Department, CSIR-Central Institute of Medicinal & Aromatic Plants, Lucknow, UP–226015, India*

E-mail: gopan@iitk.ac.in

Phone: +91 5122596830. Fax: +91 5122596806

S1: Statistical analysis of the angle between 1D islands for FcS_2C_3 and FcS_2C_4

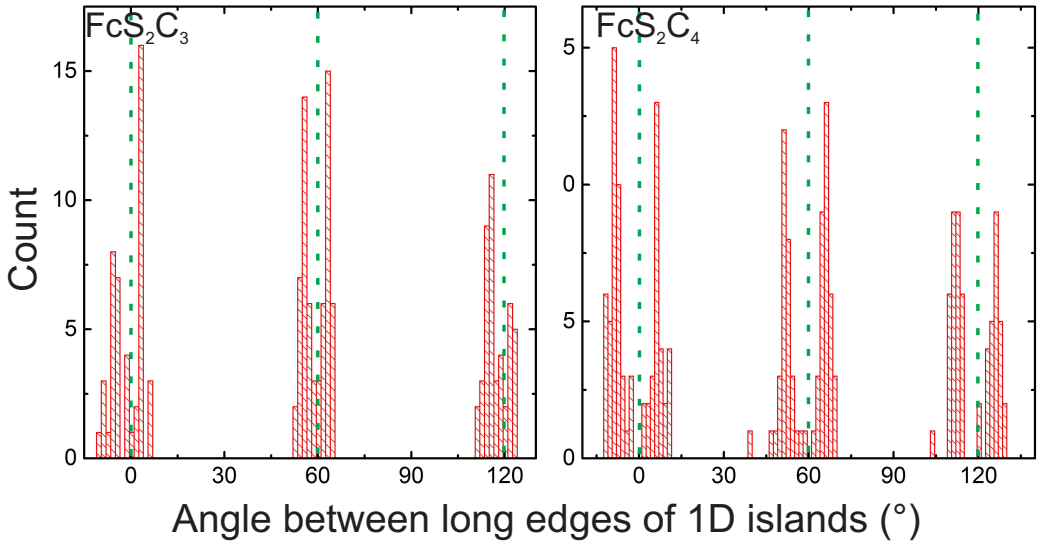

Figure S1: Statistical analysis of the angle between the long edge of several 1D islands for FcS_2C_3 and FcS_2C_4. The green dashed lines depict the graphite compact lattice directions. For FcS_2C_3 major peaks are observed at $-5/3/56/63/115/122 \pm 3°$. This distribution is observed as three pairs and the average spacing between the peaks in the pairs is $\approx 8°$. The pairs are separated by $\approx 60°$ with its adjacent pairs reflecting the three fold graphite lattice symmetry. The pairs are suggesting that 1D islands are rotated by $\approx \pm 4°$ with respect to all graphite compact lattice directions. This is consistent with the FFT analysis in Figure S2. For FcS_2C_4 major peaks are located at $-8/7/52/66/112/126 \pm 5°$. This distribution is also observed as three pairs similar as in FcS_2C_3 and the average spacing between the peaks in the pairs is $\approx 15°$. It indicates that the 1D islands are rotated by $\approx \pm 7.5°$ with respect to all graphite compact lattice directions. In this context, it is important to mention that after drop-casted solution of FcS_2C_3 and FcS_2C_4 from each and every solvent, the orientation of the 1D islands with respect to graphite lattice directions appeared to be similar for all cases on surface.

S2: 2D-FFT of high coverage areas of ultra-thin film of FcS_2C_3

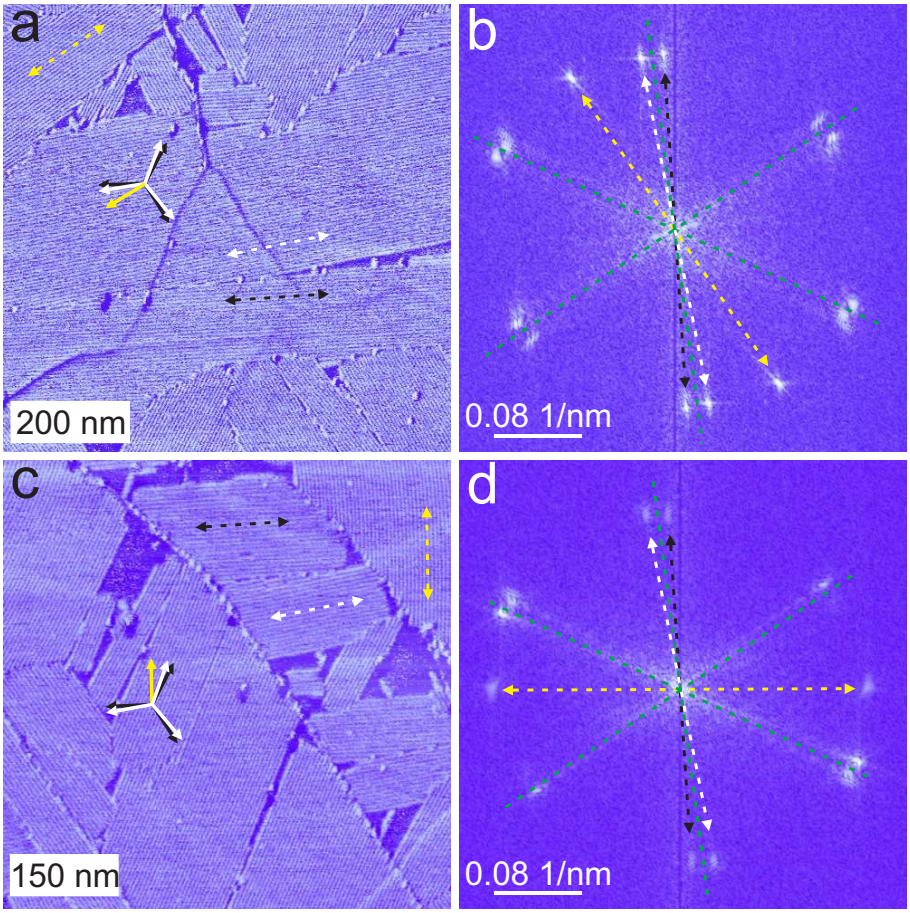

Figure S2: (a) and (c) are AFM phase images of two independent high coverage areas ($\approx 1ML$) of ultra-thin film of FcS_2C_3 on HOPG (0001) deposited from methanol and the corresponding 2D–FFT images are included in (b) and (d). Arrows indicate different types of growth of molecules on surfaces as evident from the line like contrast, which is also reflected in the FFT. Two types of growth are observed; first with molecular rows aligned by $\approx \pm 4°$ (white and black arrows) and other types with $\approx \pm 26°$ (yellow arrows) with respect to all graphite lattice directions. Green dashed lines depict the graphite compact lattice directions as obtained from the orientations of islands.

S3: Growth facet angle of 1D islands of FcS_2C_3 obtained from different solvents

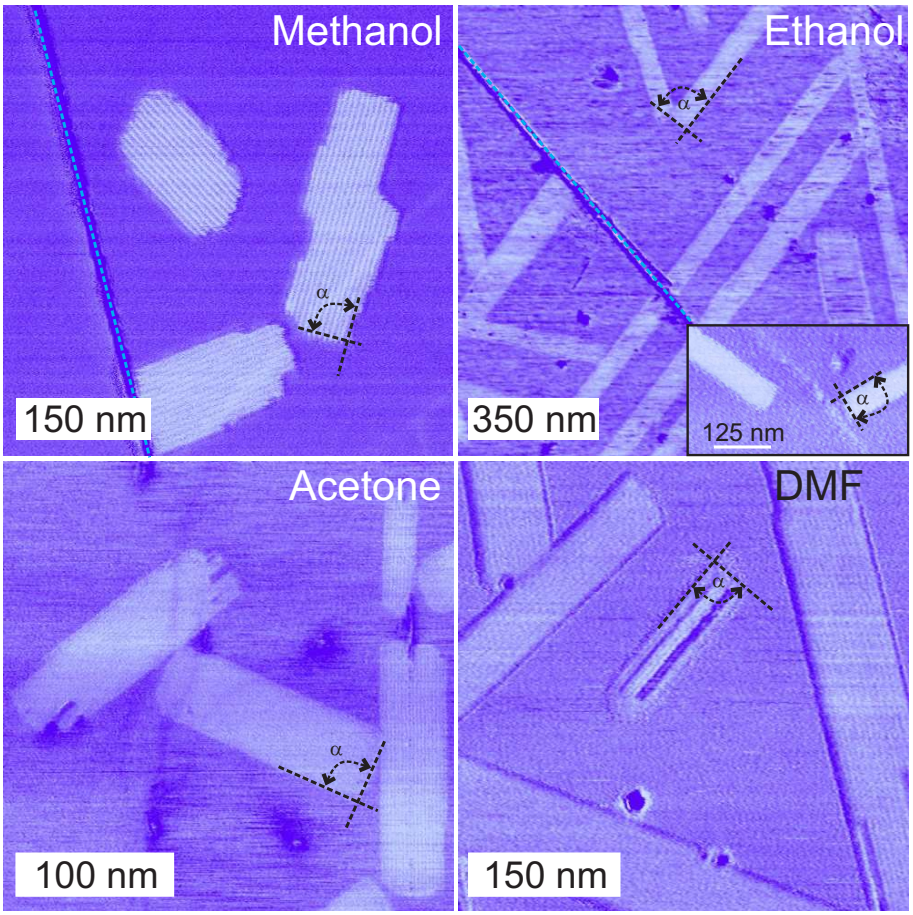

Figure S3: AFM phase images of ultrathin film of FcS_2C_3 depicting highly resolved 1D islands on HOPG obtained from methanol, ethanol, acetone and DMF. Facet angle of growth of 1D isands is shown by $\alpha \approx 90°$.

S4: Additional AFM data showing exclusive 1D islands of FcS_2C_3

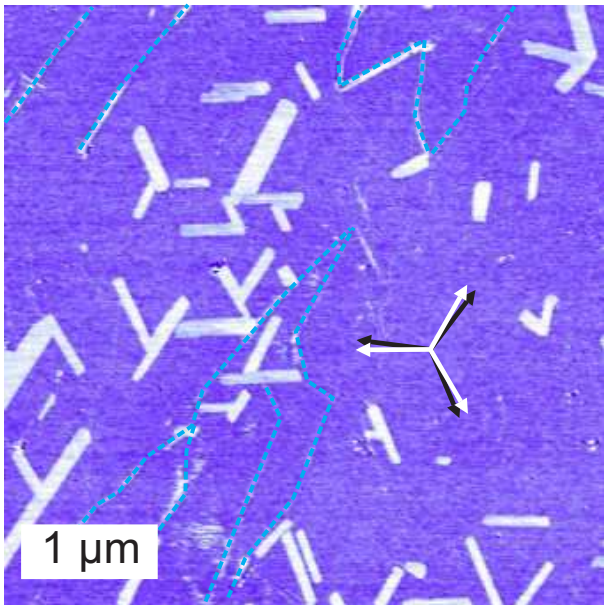

Figure S4: Additional AFM phase image depicting region with only 1D islands. White and black arrows indicate the growth directions of 1D islands with respect to graphite compact lattice directions.

S5: AFM topographs of the corrosponding phase images in Figure 3

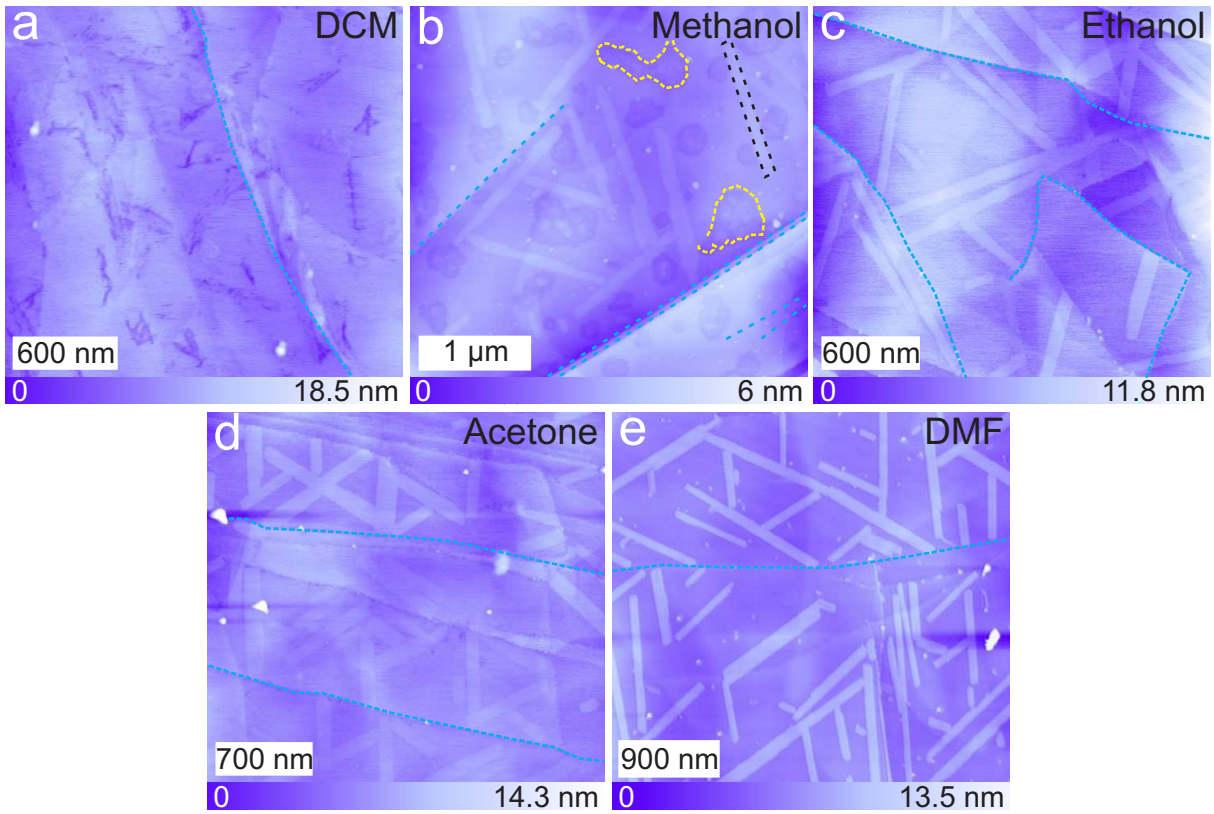

Figure S5: The corresponding AFM topographs of phase images shown in Figure 3. Phase images are included in the manuscript due to the fact that the molecular islands are clearly discerned with respect to the graphite terrace. This is rather difficult in topograph because of multi-atomic terraces as evident from Z scale. A few terrace edges are indicated with blue dashed lines.

S6: STM topographs of ultrathin film of FcS_2C_3

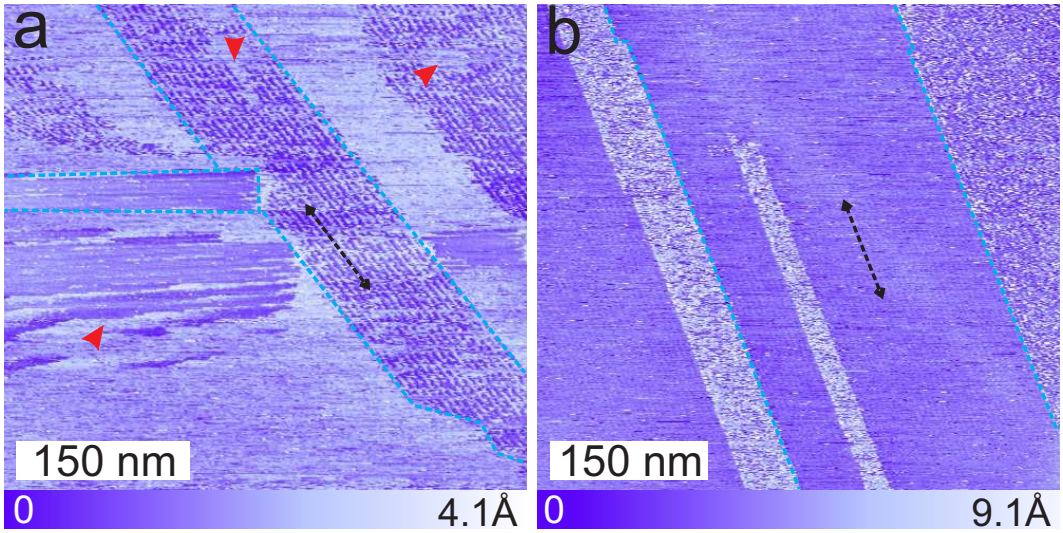

Figure S6: Constant current STM topographs of two independent areas of ultra-thin film of FcS_2C_3 on HOPG (0001) surface deposited from methanol. Tunneling parameters are 50 pA, 0.2 V for (a) and 30 pA, 0.6 V for (b). Molecular island edges are marked with blue dashed line and the shape of the islands are indicating that they are most likely similar to the 1D islands observed using AFM. The molecular island edges are extremely dynamic while scanning and is dependent on the scanning voltage. Due to the dynamic nature of islands while scanning we could not resolve sub-molecular details. However, a line like contrast is observed in both images (marked with double headed arrows) and are spaced by 5.9 ± 0.1 nm. This spacing corresponds to the super-periodicity $\boldsymbol{S}$ observed for 1D islands using AFM.

S7: AFM images and corrosponding model for ultrathin film of FcS_2C_4

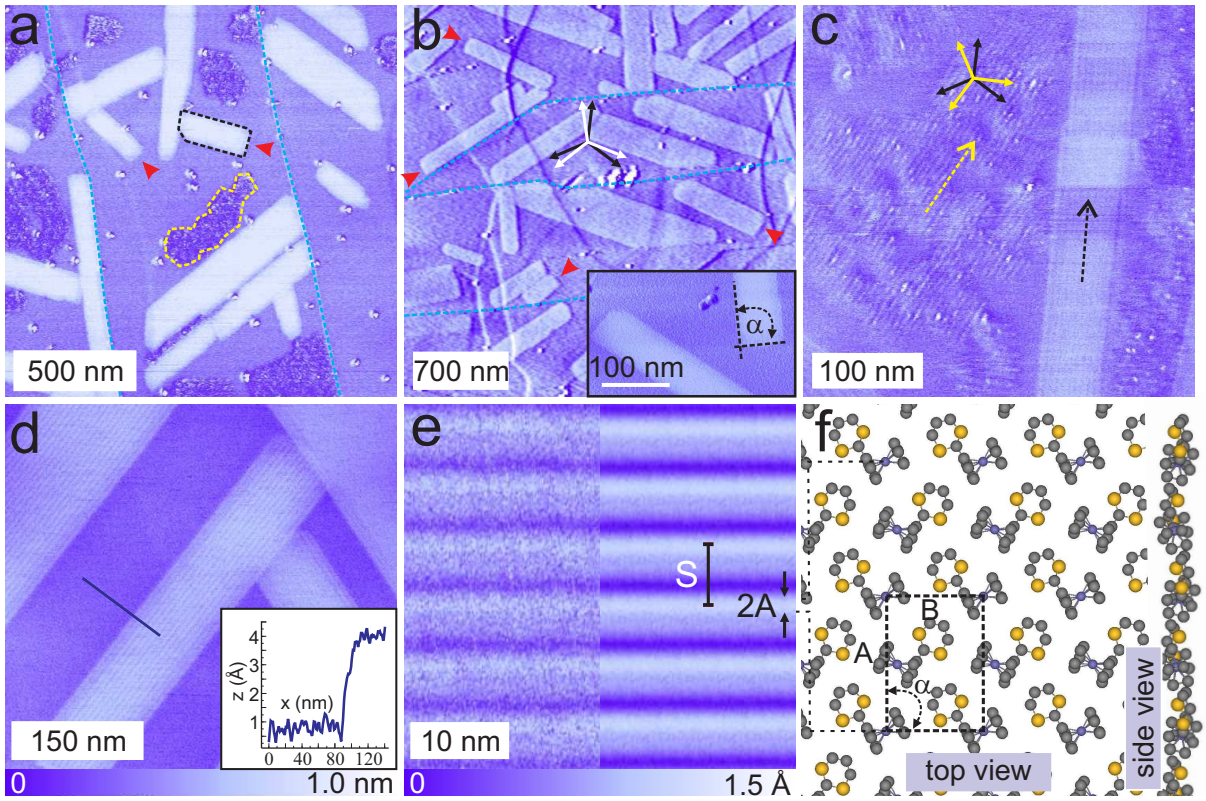

Figure S7

(a) Constant-force AFM phase image of ultrathin film of FcS_2C_4 on HOPG (0001) surface deposited from methanol. Two types of domains are indicated with dashed black (1D) and yellow (2D) lines. Dashed blue lines are indicating few terrace edges. (b) AFM phase image depicting region covered solely with 1D islands. All possible growth directions of 1D islands (long edge) with respect to graphite compact directions are marked with white and black arrows. The islands are rotated by $\approx \pm 7.5°$ with respect to the graphite lattice directions (refer Figure S1). The red arrow heads are indicating the growth facet of a few 1D islands, which is $\approx 90°$. Inset shows facet of few 1D islands with α as facet angle. (c) High resolution phase image of coexisting 1D and 2D islands; their relative orientations are marked with black and yellow arrows, respectively. The 2D islands (yellow arrows) are rotated by $\approx 30°$

with respect to each other. This indicates that these islands are rotated by $\approx 30^\circ$ with respect to grahite compact lattice directions. This assignment is made from the relative orientation of 2D and 1D islands, where 1D islands are only rotated by $\approx \pm 7.5^\circ$ with respect to the graphite lattice directions.

(d) Topograph showing 1D islands and height profile of a 1D island. (e) Highly resolved topograph of part of a 1D island; right half of the image is averaged (using grid). (f) Tentative model for the molecular packing in ultra-thin film of FcS_2C_4 on surface is proposed using the same method that was used for FcS_2C_3. Interestingly FcS_2C_4 also packs as layered structure in the crystal with the space group $P2_1/a$ (CCDC 1026923).[S1] The layer encompassing the most favorable interactions in bulk packing is depicted in Figure S7f. Unit cell is marked with a black dashed rectangle with $\boldsymbol{A}$, $\boldsymbol{B}$ as lattice parameters. The angle enclosed between $\boldsymbol{A}$, $\boldsymbol{B}$ is 90°. The layer is stabilized by $\pi \cdots$H–C– interaction[S2–S4] between one of the Cp rings and hydrogen of the dithiane ring. The growth facet and spacing between the molecular rows are further used as evidences for confirming the packing of molecules on surface to the above model. The growth facet ($\approx 89^\circ$, indicated using α in Figure S7b) is comparable to the angle between $\boldsymbol{A}$, $\boldsymbol{B}$ in the model.[S5] The spacing between the line-like rows (indicated by $\boldsymbol{2A}$) in 1D islands is 2.9 ± 0.2 nm which is two times that of the spacing between the molecular rows. The observed superstructure originating from Moiré effect (see Figure S7e) is spaced by 6.1 ± 0.2 nm (marked with $\boldsymbol{S}$).[S6] The apparent height of FcS_2C_4 is 0.3 nm lower (height profile in Figure S7d) than that of FcS_2C_3, which is consistent to the dithiane group oriented parallel to the surface, while the dithiolane group of FcS_2C_3 is pointing away from the surface (see the side view in Figure S7f).

S8: STM images and the corrosponding 2D-FFT of ultrathin film of FcS_2C_4

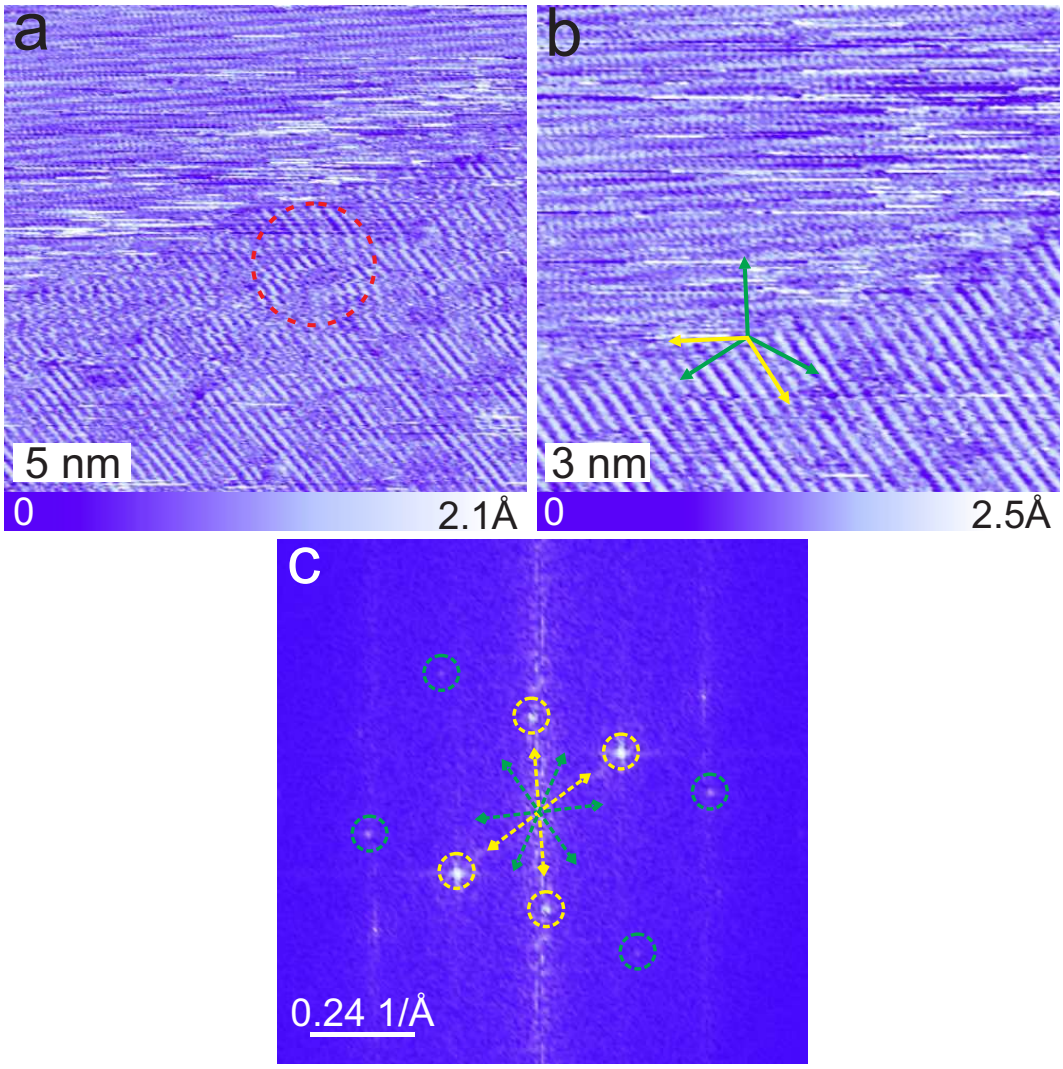

Figure S8

Figure S8 (a) and (b) are constant current STM topographs of ultra-thin film of FcS_2C_4 on HOPG (0001) surface deposited from methanol. Tunneling parameters are 30 pA, 0.1 V for both (a) and (b). Molecular islands are resolved as line like contrast most likely arising due to adjacent molecular rows (marked with yellow arrows). (c) 2D-FFT of (b) is showing different growth directions of molecular rows (indicated with yellow dashed arrows) and are spaced by 0.5 ± 0.1 nm. The spacing between the molecular rows corresponds to

half of the lattice vector ($\boldsymbol{A}$) in the model predicted in Figure S7, which confirms that these line like contrast is originating from adjacent molecular rows. The graphite lattice directions are observed both in STM topographs and 2D-FFT and are indicated by green dashed lines. The molecular rows are rotated with respect to all graphite compact lattice directions by $\approx 30°$. This is consistent to the results obtained using AFM (refer Figure S7). Unfortunately the imaging of these islands was very sensitive due to instabilities during the scanning (example marked using red circle in (a)) and thus we could not resolve further sub-molecular details. The instabilities are most likely due to weak interaction of molecule with substrate. With AFM, however, such behavior is not observed most likely due to the mode of scanning (soft tapping mode). Therefore we are using the combined STM and AFM results to predict a model for the adlayer. The proposed model is based on the bulk packing and several geometrical parameters obtained from AFM and STM. The adsorption geometry of Fc within this model is comparable to that proposed in previous literature.[S2–S4]

S9: Solubility of FcS_2C_3 and FcS_2C_4

Solvent	FcS_2C_3 (mg/mL)	FcS_2C_4 (mg/mL)	Dipole moment (D)
Methanol	10.0	12.5	1.7
Ethanol	15.5	18.5	1.69
Acetone	60	62	2.85
DMF	84	88	3.86
DCM	320	340	8.93

The solubility of FcS_2C_3 and FcS_2C_4 shows a good agreement with the dipole moment of the solvents. With increasing dipole moment, the solubility of both molecules enhanced many folds. There is a direct corelation between extent of solubility and the dipole moments between these Fc derivatives. FcS_2C_4 which has higher dipole moment (2.23 D) than FcS_2C_3 (1.17 D) exhibits higher degree of solubility.

S10: Synthetic details of FcS_2C_3

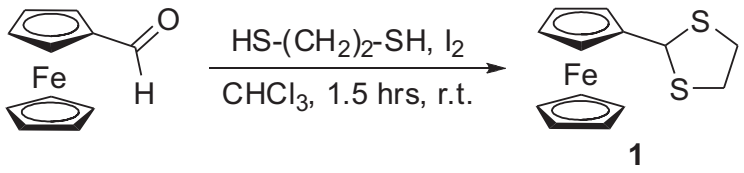

Figure S9: Synthesis of 2-Ferrocenyl-1,3-dithiolane (1, FcS_2C_3)

To a stirred solution of ferrocenecarboxaldehyde (0.214 g, 1 mmol) and 1,2-ethanedithiol (0.92 mL, 1.1 mmol) in dry CH_3Cl (20 mL), catalytic amount of iodine (0.025 g, 0.2 mmol) was added. The reaction mixture was stirred for 1 h and then quenched by 20 mL saturated $Na_2S_2O_3$ solution and was extracted with $CHCl_3$ (2 x 20 mL). The organic layers were combined and was washed with 10 % KOH solution (1 x 20 mL) and then with water (1 x 20 mL). The solution was dried over anhydrous Na_2SO_4 and concentrated under vacuum. The crude product was recrystallized from a solution in hexane and dichloromethane (10:1), to get orange crystals (0.265 g, 91 %); Mp: 92-93 ^oC; IR (KBr): 3089, 2962, 2917 cm^{-1}; ^1H NMR ($CDCl_3$, 500 MHz): δ 5.59 (s, 1H), 4.32 (m, 2H), 4.20 (s, 5H), 4.18 – 4.16 (m, 2H), 3.42 – 3.35 (m, 2H), 3.30 – 3.23 (m, 2H) ppm; ^{13}C NMR ($CDCl_3$, 125 MHz): δ 84.04, 64.40, 63.72, 62.90, 48.48, 35.09 ppm; HRMS (ES): m/z calculated for $C_{13}H_{14}FeS_2$ [M+]: 289.9886; found: 289.9885.[S7]

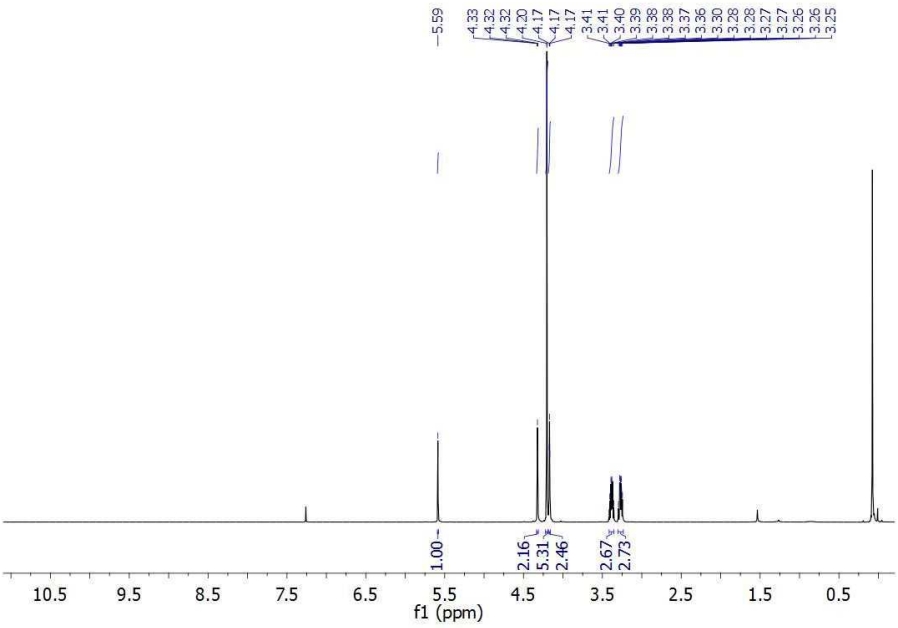

Figure S10: ^{1}H NMR (500 MHz) of FcS_2C_3 in $CDCl_3$.

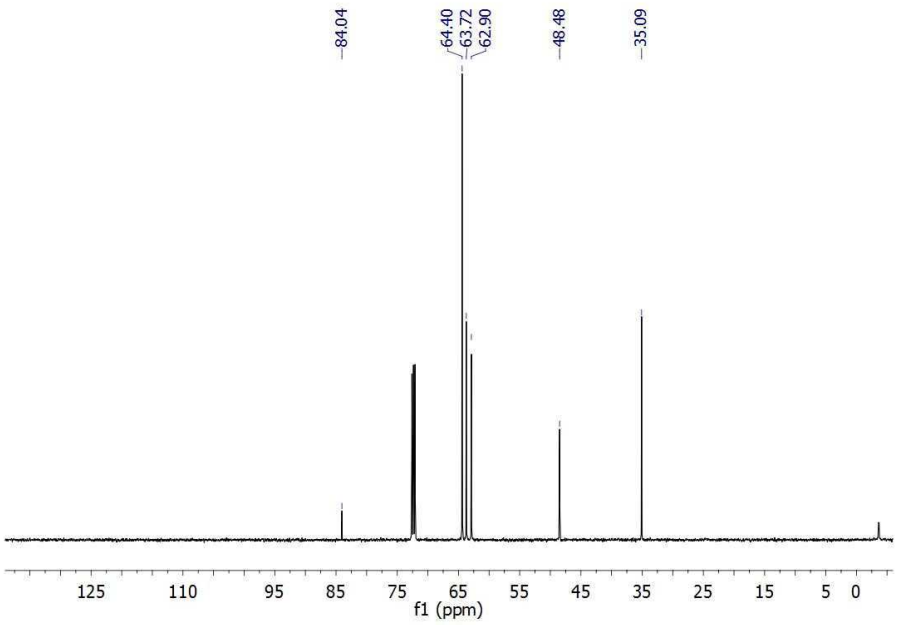

Figure S11: ^{13}C NMR (125 MHz) of FcS_2C_3 in $CDCl_3$.

S11: Crystal structure refinement parameters for FcS_2C_3

Molecular formula	$C_{13}H_{14}FeS_2$	F(000)	600
Mr	290.2	μ (mm^{-1})	1.574
Crystal system	Monoclinic	θ range for data collection (^{o})	3.186 – 28.273
Space group	$P2_1/c$	Reflections collected	6082
a (Å)	14.6365 (5)	Unique reflections	2933
b (Å)	8.9040 (3)	Observed reflections [I > 2σ(I)]	2737
c (Å)	9.1925 (4)	R(int)	0.0156
β (^{o})	91.612 (1)	Goodness-of-fit on F^2	1.021
Volume ($Å^3$)	1197.5 (1)	R1 and wR2 [I > 2σ(I)]	0.0210 and 0.0506
Z	4	R1 and wR2 (all data)	0.0233 and 0.0516
Dx (Mg m^{-3})	1.610	$\Delta\rho_{max}$ and $\Delta\rho_{min}$ ($eÅ^{-3}$)	0.324 and -0.356
T (K)	100	No. of parameters	145

Single crystals of FcS_2C_3 were obtained from four different solvent systems, hexane-dichloro methane, acetone, methanol and ethanol by slow evaporation. Regardless of the solvent system used for crystallization, all the experiments yielded crystals with similar unit cell parameters. Single-crystal X-ray data were collected at 100 K on a Bruker SMART APEX CCD diffractometer using graphite monochromated MoKα radiation (λ = 0.71073 Å). Data were acquired using a combination of ϕ and ω scans. The structure was solved by direct methods using SHELXS and was refined against F^2 with full-matrix least squares method by using SHELXL–2014. Anisotropic refinement was performed on all the non-hydrogen atoms. Hydrogen atoms were geometrically fixed in idealized positions and were refined as riding over the atoms to which they were bonded.

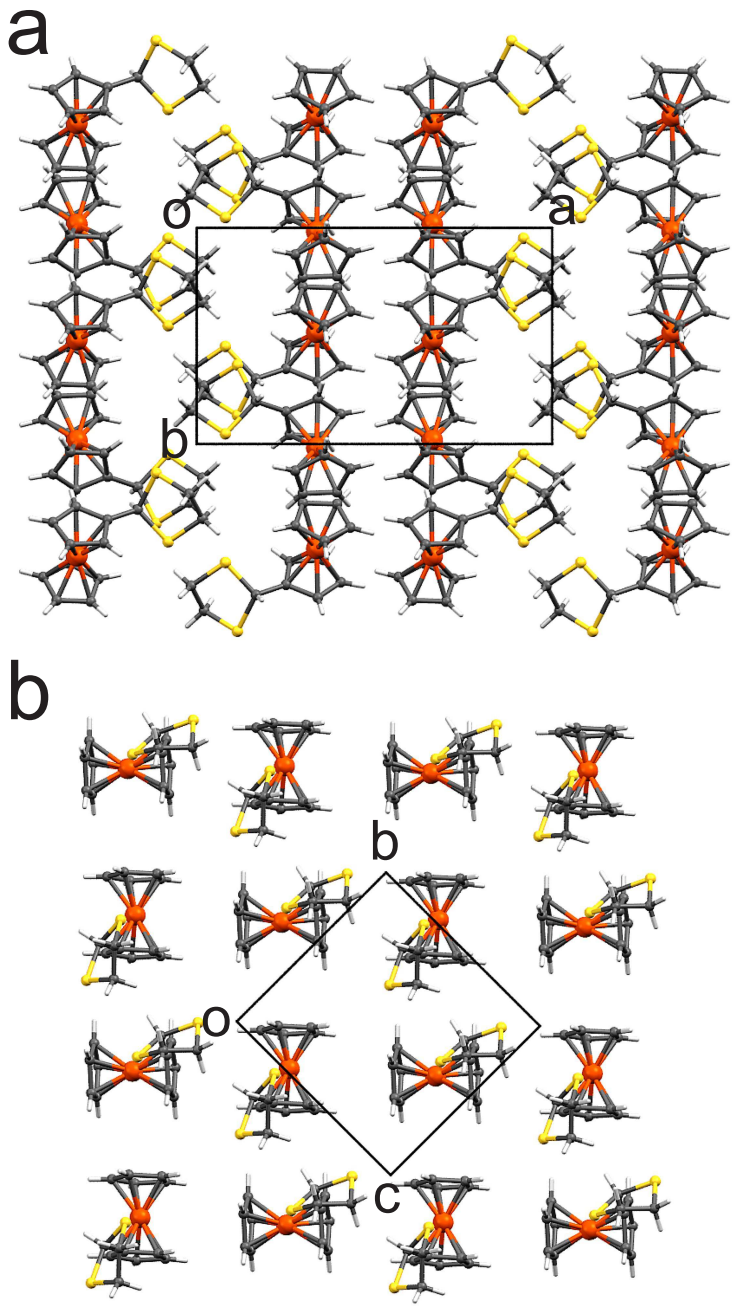

Figure S12: Packing of FcS_2C_3 molecules in crystals. (a) View down the crystallographic c-axis. (b) View down the crystallographic a-axis, showing the 2D layer of molecules held together by aromatic interaction between cyclopentadienyl rings.

References

(S1) Philip, A. T.; Chacko, S.; Ramapanicker, R. *J. Pept. Sci.* **2015**, *21*, 887 – 892.

(S2) Hartmann, S.; Winter, R. F.; Scheiring, T.; Wanner, M. *J. Organomet. Chem.* **2001**, *637-639*, 240 – 250.

(S3) Bogdanović, G. A.; Novaković, S. B. *CrystEngComm* **2011**, *13*, 6930 – 6932.

(S4) Verma, S. K.; Singh, V. K. *J. Organomet. Chem.* **2015**, *791*, 214 – 224.

(S5) Only islands ending on free terraces are used for the measurement. 1D islands ending on terraces, kinks and other islands are discarded due to the fact that the edges acquires the shapes of the terraces, kinks and other islands.

(S6) Saha, P.; Yadav, K.; Chacko, S.; Philip, A. T.; Ramapanicker, R.; Gopakumar, T. G. *J. Phys. Chem. C* **2016**, *120*, 9223 – 9228.

(S7) Firouzabadi, H.; Iranpoor, N.; Hazarkhani, H. *J. Org. Chem.* **2001**, *66*, 7527–7529.